

$\langle 310 \rangle$ misfit dislocations in ZnSe/GaAs(001) heterostructure

This article has been downloaded from IOPscience. Please scroll down to see the full text article.

2002 J. Phys.: Condens. Matter 14 13291

(<http://iopscience.iop.org/0953-8984/14/48/380>)

View [the table of contents for this issue](#), or go to the [journal homepage](#) for more

Download details:

IP Address: 171.66.16.97

The article was downloaded on 18/05/2010 at 19:17

Please note that [terms and conditions apply](#).

$\langle 310 \rangle$ misfit dislocations in ZnSe/GaAs(001) heterostructure

S Lavagne, C Levade and G Vanderschaeve

CEMES-CNRS, 29 rue Jeanne Marvig, BP 4347, Toulouse cedex 4, France

and

INSA, Physics Department, 135 avenue de Rangueil, 31077 Toulouse cedex 4, France

Received 27 September 2002

Published 22 November 2002

Online at stacks.iop.org/JPhysCM/14/13291

Abstract

Strain relaxation in ZnSe/GaAs(001) heterostructure grown by molecular beam epitaxy is studied by transmission electron microscopy. In as-grown samples, an array of perfect misfit dislocations, lying along $\langle 310 \rangle$ directions, with Burgers vector $(1/2)\langle 011 \rangle$ inclined to the interface is observed. The corresponding threading segments propagate by glide in $\{331\}$ planes, leaving misfit segments in the interface.

From a mechanical equilibrium analysis, it is concluded that, in the case of low misfit (0.27%), the critical thickness for $\{331\}$ planes is less than for $\{111\}$ glide. Dislocations with the $(1/2)\langle 011 \rangle$ Burgers vector lying along $\langle 310 \rangle$ directions are more efficient at relaxing the misfit strain than dislocations lying along $\langle 110 \rangle$ directions.

1. Introduction

Stress relaxation in a strained heterostructure occurs via the formation of a network of misfit dislocations in the layer–substrate interface. It is generally assumed that the driving force for such a phenomena is activation of $(1/2)\langle 110 \rangle\{111\}$ slip systems in the layer, as it is well known that these systems are operative in bulk semiconductors. Note, however, that the glide process in the $\langle 110 \rangle\{110\}$ system has been observed in heterostructures with relatively high misfit ($>6\%$) (see Albrecht *et al* 1992).

In this paper it is shown that early stages of stress relaxation in ZnSe/GaAs(001) heterostructure proceed by activation of secondary $(1/2)\langle 011 \rangle\{133\}$ slip systems. The efficiency of such a relaxation process is discussed following the mechanical analysis of Albrecht *et al* (1993).

2. Experimental details

ZnSe/GaAs heterostructures were grown by molecular beam epitaxy at 280 °C in CRHEA, Valbonne (France), with an excess of Se (Bousquet *et al* 1998). The layer was 2500 Å thick.

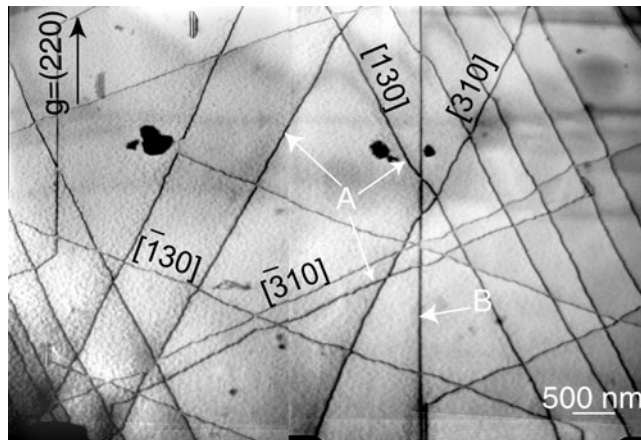


Figure 1. TEM images of misfit dislocations. The sample thickness is 2200 Å. Most of the dislocations are aligned along unusual $\langle 310 \rangle$ directions.

X-ray measurements indicate a slight tetragonality of the ZnSe film, suggesting that it is not completely relaxed. As the lattice parameter of bulk ZnSe is slightly larger than that of GaAs (misfit 0.27%), the layer was in compression.

Transmission electron microscopy (TEM) plan-view samples were processed from the back (Lavagne *et al* 2000): mechanical polishing followed by chemical etching of the GaAs substrate. The final ion beam was not used, to avoid the formation of 'speckles' on the TEM images. The TEM experiments were performed in a JEOL 2010 operating at 200 keV.

As the sphalerite structure is non-centrosymmetric, the absolute polarity of the crystal had to be determined. Recently, a novel method has been used (Lavagne *et al* 2002): convergent beam electron diffraction by $\{001\}$ plan-view samples. As for $\{110\}$ cross-section samples, it is based on the occurrences of constructive or destructive interferences in the $\pm(200)$ discs (Taftø and Spence 1982).

3. TEM observations

Figure 1 shows a large area of a ZnSe/GaAs sample interface. An array of long misfit dislocations can be seen. Most of them (marked A) present little undulations, whereas the others (B) are very straight. The former ones lie along unusual $\langle 310 \rangle$ directions; the latter ones lie along the low-energy directions $\langle 110 \rangle$. In the following we concentrate on the characterization of those misfit dislocations lying along $\langle 310 \rangle$ directions.

They originate from multitwinned zones in the layer, which are probably due to growth heterogeneities (Lavagne 2002).

Threading segments are sometimes observed (figure 2), which suggests that these misfit dislocations extend into the interface by dislocation glide.

As reported in previous studies and in similar material (see for example Petruzzello *et al* 1988, Ruvimov *et al* 1996), misfit dislocations have the Burgers vector $(1/2)\langle 011 \rangle$, inclined to the interface. Figure 3 shows a TEM analysis of a particular dislocation lying along $[130]$, marked with an arrow. It is in contrast when imaged with the (220) reflection (figure 3(a)) and out of contrast when imaged with the (040) reflection (figure 3(b)) and the (111) reflection (figure 3(c)). This indicates that the Burgers vector of this dislocation is $b = (1/2)[101]$. Note that all dislocations lying along a given $\langle 310 \rangle$ direction have the same Burgers vector. Taking

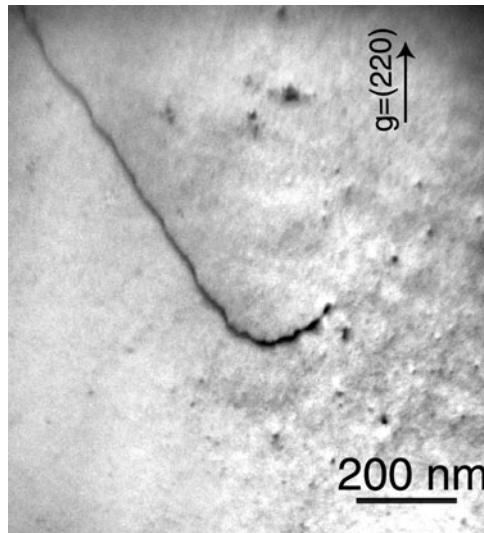


Figure 2. A threading segment on a $\langle 310 \rangle$ misfit dislocation.

into account the line direction and the Burgers vector, this indicates that the glide plane of the threading segment is the $(31\bar{3})$ plane. A systematic analysis of all the misfit dislocations leads to the conclusion that they extend by glide in a secondary $\{3\bar{3}1\}$ plane.

Note that these dislocations do not appear dissociated, even under weak-beam conditions. Nevertheless, a frequent observation is that the threading segment could interact with a pre-existing triangular stacking fault to give a widely dissociated stacking fault ribbon in the $\{111\}$ plane (figure 4). This suggests that the threading segment in the $\{3\bar{3}1\}$ could cross-slip in a $\{111\}$ plane, when it is subjected to interactions with other defects. The observation of a sudden change in line direction of the misfit dislocations from $\langle 310 \rangle$ to $\langle 110 \rangle$ (Lavagne *et al* 2000) is another indication of this effect.

4. Discussion

4.1. The nature of the glide process

Most of the dislocations lie along unusual $\langle 310 \rangle$ directions in the interface plane, which are not the lowest-energy line directions in the sphalerite structure. Previous studies have already reported an irregular network consisting of dislocations parallel to $\langle 100 \rangle$ directions in the ZnSe/GaAs heterostructure (Guha *et al* 1992, Kuo *et al* 1993), but to our knowledge $\langle 310 \rangle$ directions have never been observed in this material.

It is suggested that the formation of these misfit dislocations is related to the activation of secondary $(1/2)\langle 011 \rangle\{133\}$ slip systems. This unusual slip plane could be considered as a 'composite' plane resulting from the activation of two secant $\{111\}$ planes (both containing the Burgers vector). If this was true, the mean $\langle 310 \rangle$ direction should consist of short segments lying along the two perpendicular $\langle 110 \rangle$ directions in the (001) plane. Weak-beam dark-field images at rather high magnification did not allow us to distinguish these short segments. So we may conclude that the slip distance in these two $\{111\}$ planes, if there is any slip, is rather short (lower than 3 nm).

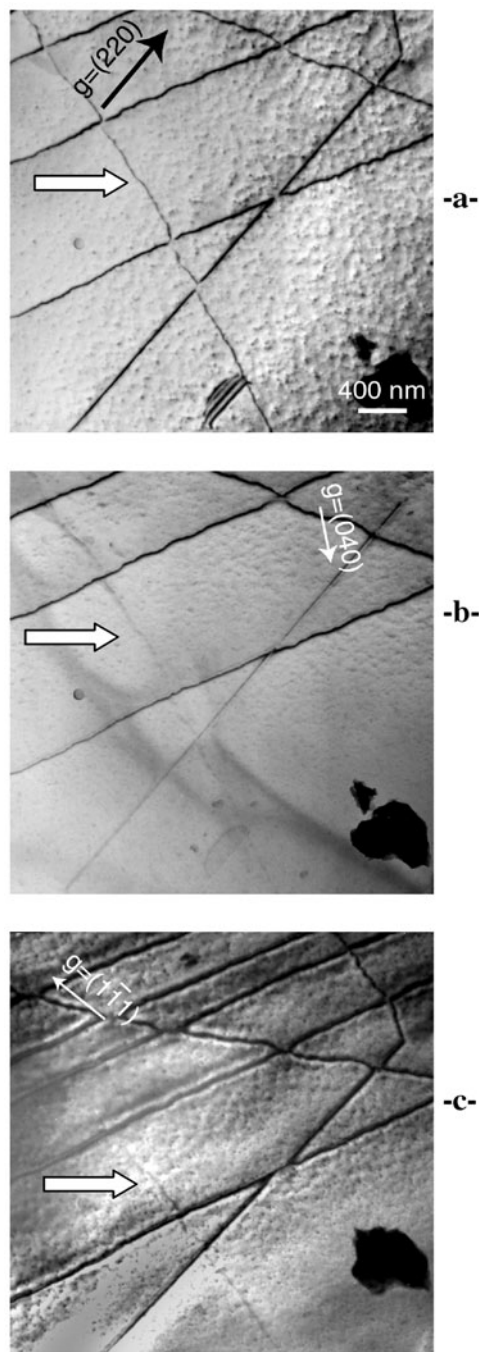


Figure 3. TEM images of a misfit dislocation under different diffraction conditions: (a) $g = (220)$; the dislocation shown by the arrow is in contrast; (b) $g = (040)$; the dislocation is out of contrast; (c) $g = (1\bar{1}1)$; the dislocation is out of contrast.

4.2. Efficiency of the strain relaxation

The efficiency of the misfit strain relaxation is related to the efficient Burgers vector component (i.e. the component of the Burgers vector in the interface plane, perpendicular to the misfit

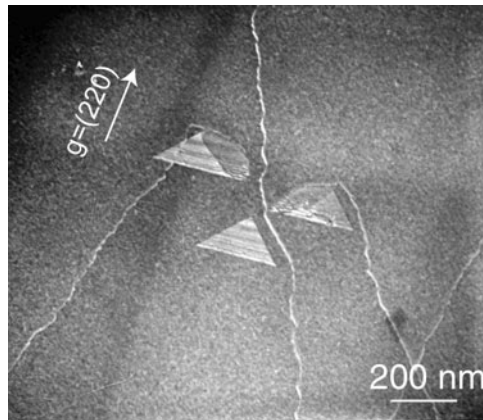


Figure 4. The interaction between a (310) threading segment and a pre-existing triangular stacking fault.

dislocation line). This efficient component is evaluated as $0.47a$ for dislocations lying along (310) directions, higher than that for dislocations lying along (110) directions (produced by glide in primary {111} planes): $0.35a$.

Taking into account the efficient component of the Burgers vector and the mean distance between interfacial dislocations, the misfit strain that is released by this network is roughly estimated as 6×10^{-4} , to be compared to the crystallographic misfit: 27×10^{-4} . This is another indication that the layer is not completely relaxed. Complete relaxation of the layer occurs during TEM *in situ* heating experiments. Heating the sample up to 250 °C under an electron beam causes the sudden formation of a grid of edge dislocations with $(1/2)\langle 110 \rangle$ Burgers vectors in the interface (see figure 5). These dislocations are very efficient for completely relaxing the misfit stress and thermal stress.

4.3. Mechanical analysis

In order to interpret the activation of the $(1/2)\langle 011 \rangle\{331\}$ glide system, we use the mechanical analysis of Matthews and Blakeslee (1974). Similar analysis has been performed by Albrecht *et al* (1993) who investigated the dislocation glide in the {110} planes. We consider first the homogeneous nucleation of a half-loop and then the extension of the dislocation by glide.

4.3.1. Nucleation energy. The activation energy for nucleation of such a loop is written as

$$E = \frac{\mu b}{8(1-\nu)} r \left[b(2-\nu) \ln \left(\frac{\alpha r}{b} \right) - 8\pi f(1+\nu)r \cos \lambda \cos \theta - 2b(1-\nu) \sin \beta \right]$$

where μ is the shear modulus, ν Poisson's ratio, b the Burgers vector of the dislocation half-loop, α the core parameter, β the angle between the Burgers vector of the misfit dislocation and its line direction, r the radius of the loop and $\cos \lambda \cos \theta$ the Schmid factor.

It is calculated from an energy balance between the stress relief, dislocation line energy and surface energy of the corresponding surface step.

In figure 6 a comparison is shown between the activation energies for forming a glide half-loop dislocation with Burgers vector $(1/2)\langle 011 \rangle$ in different planes. The activation energy for

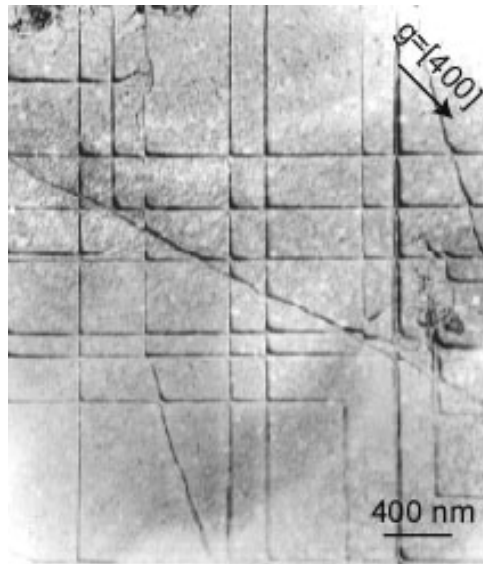


Figure 5. An orthogonal network of edge dislocations created during TEM *in situ* heating experiments.

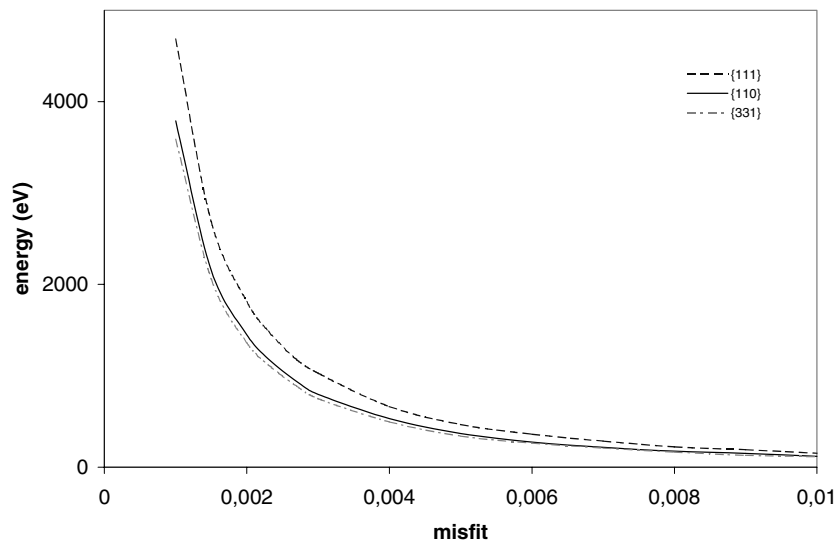


Figure 6. Nucleation energy as a function of misfit for different glide systems. $(a/2)\{110\}\{111\}$, $(a/2)\{110\}\{110\}$ and $(a/2)\{110\}\{331\}$ systems are studied.

forming a dislocation in $\{331\}$ planes is lower than for a 60° dislocation in $\{111\}$ planes and even lower than for a 90° dislocation in $\{110\}$ planes.

4.3.2. Propagation of a threading segment. The second calculation concerns propagation of a threading segment leaving a misfit dislocation in the interface. We calculate the critical thickness H for which an unstable configuration (see figure 7) is obtained—that is, when

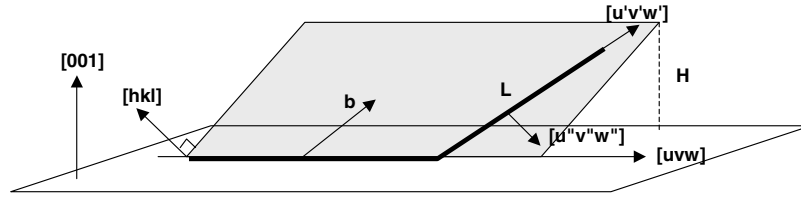


Figure 7. A schematic drawing of the glide systems.

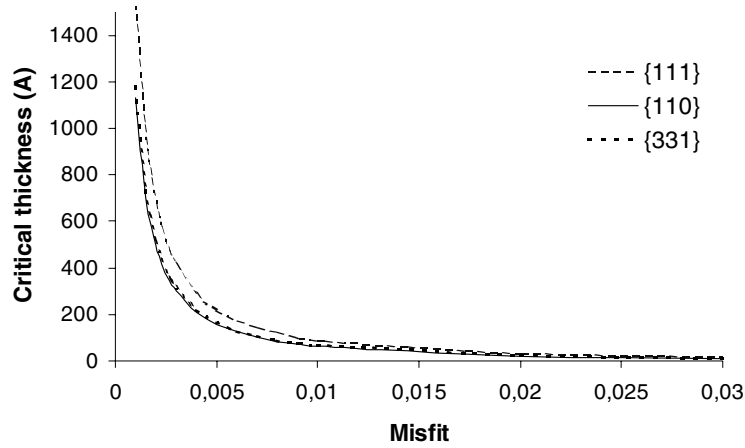


Figure 8. Critical thicknesses as a function of misfit and glide system: $(a/2)\langle 110\rangle\{111\}$, $(a/2)\langle 110\rangle\{110\}$ and $(a/2)\langle 110\rangle\{331\}$ systems.

the Peach and Kohler force on the threading segment exceeds the line tension of the misfit dislocation in the interface.

We obtain

$$H = \frac{b}{8\pi f \chi} \frac{(1 - \nu \cos^2 \beta)}{(1 + \nu)} \left(\ln \frac{H}{b} + 1 \right)$$

with χ a geometrical factor:

$$\chi = \frac{l}{\sqrt{2(h^2 + k^2 + l^2)}} \frac{(uu'' + vv'' + ww'')(\sqrt{u'^2 + v'^2 + w'^2})}{w' \sqrt{u^2 + v^2 + w^2} \sqrt{u''^2 + v''^2 + w''^2}}$$

Calculations are performed without taking the lattice friction into account. In that case, the calculated critical thickness does not depend on the orientation of the threading segment in the glide plane. Results are presented in figure 8. Again, propagation in $\{331\}$ planes is favoured with respect to that in the classical $\{111\}$ planes. Note that the critical thicknesses for the $\{331\}$ and $\{110\}$ planes are very close.

The Peierls stress has been calculated following Chidambarrao *et al* (1990), for the three glide systems: it is very high for the $\{331\}$ system, and rather low for $\{111\}$ and $\{110\}$. Nevertheless, we do not believe that lattice friction plays an important role in this case. Indeed in the temperature range 250–300°C, the yield stress of bulk ZnSe crystals is not very dependent on temperature. Possibly, for thicker samples, glide in $\{111\}$ planes is favoured compared to glide in $\{331\}$ planes. Indeed, in a 5000 Å thick sample, misfit dislocations lie along $\langle 110\rangle$ directions, rather than along $\langle 310\rangle$ directions as shown in figure 9.

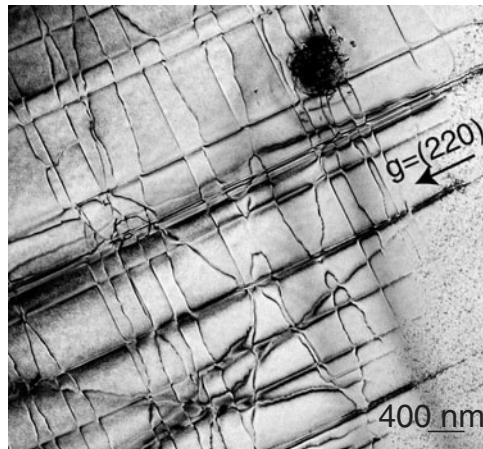


Figure 9. Misfit dislocations in 5000 Å sample thickness. Most of the dislocations are aligned along the $\langle 110 \rangle$ direction.

5. Conclusions

The early stages of plastic relaxation in a low-misfit ZnSe/GaAs heterostructure proceed by activation of the $(1/2)\langle 011 \rangle\{331\}$ glide system. A mechanical analysis of half-loop homogeneous nucleation and propagation of threading segments indicates that activation of such a secondary slip system requires less energy than that of the usual $(1/2)\langle 011 \rangle\{111\}$ glide system.

References

- Albrecht M, Strunk H P, Hansson P O and Bauser E 1992 *Proc. Mater. Res. Soc.* **238** 79
 Albrecht M, Strunk H P, Hull R and Bonar J M 1993 *Appl. Phys. Lett.* **62** 2206
 Bousquet V, Tournié E and Faurie J P 1998 *J. Cryst. Growth* **192** 102
 Chidambarrao D, Srinivasan G R, Cunningham B and Murthy C B 1990 *Appl. Phys. Lett.* **57** 1001
 Guha S, Munekata H, Legoues F K and Chang L L 1992 *Appl. Phys. Lett.* **60** 3220
 Kuo J M, Salamanca-Riba L, DePuydt J M, Cheng H and Qiu J 1993 *Appl. Phys. Lett.* **63** 3197
 Lavagne S 2002 *PhD Thesis* INSA Toulouse
 Lavagne S, Levade C, Roucau C and Vanderschaeve G 2002 *Phil. Mag. A* **82** 1451
 Lavagne S, Levade C, Vanderschaeve G, Crestou J, Tournié E and Faurie J P 2000 *J. Phys.: Condens. Matter* **12** 10287
 Matthews J W and Blakeslee E 1974 *J. Cryst. Growth* **27** 188
 Petruzzello B, Greenberg B L, Cammack D A and Dalby R 1988 *J. Appl. Phys.* **63** 2299
 Ruvimov S, Bourret E D, Washburn J and Liliental-Weber Z 1996 *Appl. Phys. Lett.* **68** 346
 Taftø J and Spence J C H 1982 *J. Appl. Crystallogr.* **15** 60